Hindawi
Mathematical Problems in Engineering
Volume 2019, Article ID 4368324, 10 pages
https://doi.org/10.1155/2019/4368324

Research Article

Digital Noninterleaved High-Power Totem Pole PFC Based on Internal Model Design

Fei Gao,[1,2] Rongfei Xia,[1] Yifei Chen,[1] and Yongjian Feng[1]

[1]*School of Aerospace Engineering, Xiamen University, Xiamen 361005, China*
[2]*School of Mechanical and Electrical Engineering, Guizhou Normal University, Guiyang 550025, China*

Correspondence should be addressed to Yongjian Feng; yjfeng@xmu.edu.cn

Received 4 January 2019; Accepted 11 March 2019; Published 15 April 2019

Academic Editor: Denizar Cruz Martins

When the control signal u(t) of totem pole PFC with GaN HEMTs is a function of measurable state variables, the state feedback gain matrix can be determined by applying state variable feedback control with Ackerman formula, so that the poles of closed-loop system can be allocated to the desired position. This correction method is especially beneficial to optimal system control according to performance requirements. By introducing the internal model of reference input, a state space function including the first-order and second-order differential of error is constructed; this novel controller makes controlled system track the reference input signal progressively with zero steady-state error. A 4 kW PFC prototype is designed to verify this design method.

1. Introduction

Generally, PFC control algorithm adopts PI control, which requires a lot of repeated debugging and depends on experience rather than mathematical tools. Applying the state variable feedback control, as long as the state variables used for feedback are measurable and the system control matrix of the state variable model is controllable, the position of the poles can be determined according to the performance requirements, and then the state feedback gain matrix can be determined according to the Ackerman formula, so that the poles can be allocated to the expected position. Compared with PI control, state variable feedback control can quickly determine control parameters and reduce debugging workload.

Increasing the control order can effectively improve the steady-state error of PFC. Usually PFC requires double integral control [1]. Internal model control adds internal model of reference input to the state variable feedback control, which enables the control system to track all kinds of reference input signals with zero steady-state error, including step signal, slope signal, and other persistent signals [2, 3]. A PFC control system requires both the magnitude of output voltage and the waveform of input current, so the internal model should include an integral cycle of voltage error and two integral cycles of current error. The PFC control model including internal model of second-order integral cycles and state variable feedback control matrix is a fourth-order control system, so it has four poles. Because the analysis method of second-order control system is abundant and mature, two poles $\alpha_1 \pm j\beta_1$ of high-order control system such as fourth-order control system can be set as dominant poles. As long as the other two poles $\alpha_2 \pm j\beta_2$ satisfy the condition $|\alpha_2| > 10|\alpha_1|$, the performance of fourth-order control system can be estimated by second-order control system; that is to say, when the absolute value of real part of dominant roots is only 1/10 or less than the nondominant, the response of the second-order system determined by the dominant roots can be used to replace the response of the higher-order system [4, 5]. In this way, the empirical formula of the second-order system can be used to determine the damping ratio and natural frequency according to the requirements of overshoot and adjusting time, so as to determine the dominant poles.

The key problem in the design of state variable feedback controller is whether the poles of the closed-loop system can be arbitrarily allocated on the s-plane. These poles of the closed-loop system are actually the eigenvalues of the system matrix of the state variable control model. If

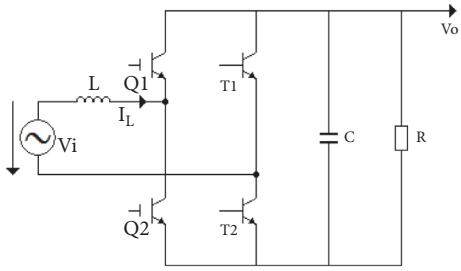

(a) Topology of digital high-power totem pole PFC

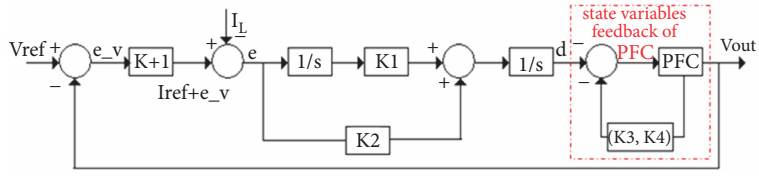

(b) Algorithm of digital high-power totem pole PFC

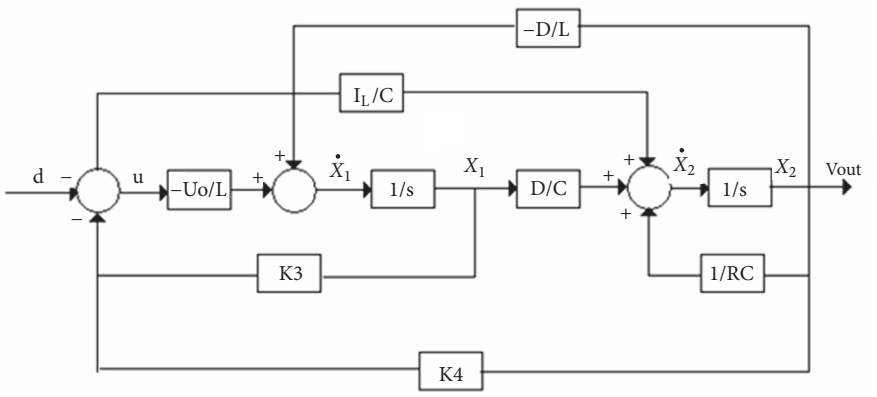

(c) The detailed diagram of state variables feedback of PFC

Figure 1: Topology and algorithm of digital high-power totem pole PFC.

the system matrix can be controlled, the closed-loop poles can be allocated to the desired position according to the performance requirements. The design of state feedback control law usually depends on poles assignment method known as state feedback gain matrix [6, 7]. The concept of controllability was proposed by Rudolph Kalman in 1960s [8–10]. Modern control technology can deal with systems whose state vectors are not completely controllable, but the linear combination of those state vectors or state vectors that cannot be controlled should be stable in nature. Such systems are called stabilizable systems. When the system is fully controllable, the system must be stabilizable. Other more complex state variable design methods can be applied to deal with stabilizable systems, such as Kalman state space decomposition. By using this method, the linear combination of state vectors or state vectors can be decomposed into two kinds of variables [3, 11], which are controllable and uncontrollable, so that the uncontrollable subspaces can be separated. For the uncontrollable subspace, the design of the control system can also be carried out theoretically. Modern control technology can also deal with systems whose state vectors are not completely observable, as long as the linear combination of those state vectors or state vectors that cannot be observed should be essentially stable; such systems are called detectable systems. When the system is fully observable, the system must have the detection ability. Observable controller can be designed to estimate the state variables. Similarly, the Kalman state space decomposition method can be applied to deal with the incomplete observable detection system. The state variables of the detection system can be decomposed into observable and nonobservable variables, so that the nonobservable subspace can be separated. For the nonobservable subspace, the control system design can also be theoretically done. For digital high-power totem pole PFC with GaN HEMTs, the control system model is controllable and all state variables are measurable, so it is not necessary to consider the design of observers.

When the power of PFC with Si MOSFETs is higher than 2 kW, interleaved structure is recommended [12–14] for the sake of reducing component stress and EMI [15, 16], while applying GaN HEMTs, high-power PFC without interleaved structure could achieve better performance [1]. It should be noted that the control method applied to a noninterleaved PFC is the same as the one applied to an interleaved PFC, as long as the boost converter cells of an interleaved system operate in phase-shift mode. Therefore, the control method of internal mode could be applied not only in a noninterleaved system but also in a system consisting of a group of interleaved converter cells.

2. Algorithm Design

The topology of digital high-power totem pole PFC is shown in Figure 1(a). Q1, Q2 are GaN HEMTs; T1, T2 are Si MOSFETs. Figure 1(b) is the algorithm schematic diagram of internal model design, I_L is the inductance current, V_i is the

input voltage, V_{ref} is the reference voltage, V_{out} is the output voltage, "PFC" is the state equation model of digital high-power totem pole PFC, illustrated in detail in Figure 1(c), e_v is the error between output voltage V_{out} and reference voltage V_{ref}, $K = |v_i|/V_{iRMS}$, $|v_i|$ and V_{iRMS} are the absolute value of instantaneous value and RMS values of input voltage V_i, respectively, K∗e_v is the reference current, e is the sum of current error and voltage error, and K1, K2, K3, and K4 are the coefficients of the state variable feedback controller. The key problem in designing the state variable feedback controller is to determine these coefficients. When designing the feedback control signals, e is regarded as the error to establish the internal model.

This paper only discusses the modeling and analysis of positive period of input voltage V_i. When V_i is negative, the method of modeling and analysis is similar to that of positive period of input voltage V_i.

When V_i is positive, Q1 is off, Q2 is on, and k=0, the state space equation of PFC control system is as follows.

$$\begin{aligned} \frac{di_L}{dt} &= \frac{u_i}{L} \\ \frac{du_o}{dt} &= -\frac{u_o}{\mathrm{RC}} \end{aligned} \tag{1}$$

When Q1 is on, Q2 is off, and k=1, the state space equation of PFC control system is as follows.

$$\begin{aligned} \frac{di_L}{dt} &= \frac{u_i}{L} - \frac{u_o}{L} \\ \frac{du_o}{dt} &= \frac{i_L}{C} - \frac{u_o}{\mathrm{RC}} \end{aligned} \tag{2}$$

According to (1), (2), and k, the unified state space equation of PFC control system can be obtained as follows.

$$\begin{aligned} \frac{di_L}{dt} &= \frac{u_i}{L} - k\frac{u_o}{L} \\ \frac{du_o}{dt} &= k\frac{i_L}{C} - \frac{u_o}{\mathrm{RC}} \end{aligned} \tag{3}$$

The expression of duty ratio d can be deduced by averaging k in a switching cycle.

$$\frac{1}{T}\int_{t0}^{t0+T} k\,dt = d \tag{4}$$

According to (3) and (4), the state space equation with input signal d can be written as follows.

$$\begin{aligned} \frac{di_L}{dt} &= \frac{u_i}{L} - d\frac{u_o}{L} \\ \frac{du_o}{dt} &= d\frac{i_L}{C} - \frac{u_o}{\mathrm{RC}} \end{aligned} \tag{5}$$

According to [1], when $di_L/dt = du_o/dt = 0$, the system works at a stable point. Stability state space equation (6) could be derived as follows.

$$I_L = \frac{V_o^2}{V_i R_L} \tag{6}$$

According to the perturbation theory, the control system can be linearized near the stable point, and the state variables can be decomposed into AC signals and DC signals (capital letters denote DC, small letters with superscript "~" denote AC). The linearization state space equation can be expressed as follows.

$$\begin{aligned} \frac{d\left(I_L + \tilde{i}_L\right)}{dt} &= \frac{\left(U_i + \tilde{u}_i\right)}{L} - \left(D + \tilde{d}\right)\frac{\left(U_o + \widetilde{u_o}\right)}{L} \\ \frac{d\left(U_o + \tilde{u}_o\right)}{dt} &= \left(D + \tilde{d}\right)\frac{\left(I_L + \tilde{i}_L\right)}{C} - \frac{\left(U_o + \widetilde{u_o}\right)}{RC} \end{aligned} \tag{7}$$

Ignoring the DC signal, the products of AC signal, and $\tilde{u}_i$ (when regarding $\tilde{d}$ as input signal, $\tilde{u}_i = 0$), the state space equation of PFC micro-variable signal can be derived as follows.

$$\begin{aligned} \frac{d\tilde{i}_L}{dt} &= -\frac{D}{L}\widetilde{u_o} - \frac{U_o}{L}\tilde{d} \\ \frac{d\widetilde{u_o}}{dt} &= \frac{D}{C}\tilde{i}_L - \frac{1}{\mathrm{RC}}\widetilde{u_o} + \frac{I_L}{C}\tilde{d} \end{aligned} \tag{8}$$

Assume $\tilde{i}_L = x_1$, $\widetilde{u_o} = x_2$, $y = \widetilde{u_o}$. According to (8) and $\widetilde{u_o} = (0,1) * (\tilde{i}_L, \widetilde{u_o})^T + (0) * \tilde{d}$, the system state space equation can be deduced as follows.

$$\begin{aligned} \begin{pmatrix} \dot{x}_1 \\ \dot{x}_2 \end{pmatrix} &= AX + B\tilde{d} \\ &= \begin{pmatrix} 0 & -\frac{D}{L} \\ \frac{D}{C} & -\frac{1}{\mathrm{RC}} \end{pmatrix}\begin{pmatrix} x_1 \\ x_2 \end{pmatrix} + \begin{pmatrix} -\frac{U_o}{L} \\ \frac{I_L}{C} \end{pmatrix}\tilde{d}, \\ y &= CX + D\tilde{d} = \begin{pmatrix} 0 & 1 \end{pmatrix}\begin{pmatrix} x_1 \\ x_2 \end{pmatrix} \end{aligned} \tag{9}$$

The error $e = (K+1)(u_o - Vref) - i_L$ can be linearized near the stable point; the result is as follows.

$$e = (K+1)\,\widetilde{u_o} - \tilde{i}_L \tag{10}$$

We get the two derivatives of e as follows.

$$\begin{aligned} \ddot{e} &= (K+1)\,\ddot{y} - \ddot{x}_1 = (K+1)\begin{pmatrix} 0 & 1 \end{pmatrix}\begin{pmatrix} \ddot{x}_1 \\ \ddot{x}_2 \end{pmatrix} - \ddot{x}_1 \\ &= \begin{pmatrix} -1 & K+1 \end{pmatrix}\begin{pmatrix} \ddot{x}_1 \\ \ddot{x}_2 \end{pmatrix} \end{aligned} \tag{11}$$

According to (9), (10), and (11), the state equation of the state variable control system with internal model can be constructed as follows.

$$\begin{pmatrix} \dot{e} \\ \ddot{e} \\ \dddot{x}_1 \\ \ddot{x}_2 \end{pmatrix} = \begin{pmatrix} 0 & 1 & 0 & 0 \\ 0 & 0 & -1 & K+1 \\ 0 & 0 & 0 & -\dfrac{D}{L} \\ 0 & 0 & \dfrac{D}{C} & \dfrac{1}{\mathrm{RC}} \end{pmatrix} \begin{pmatrix} e \\ \dot{e} \\ \ddot{x}_1 \\ \dot{x}_2 \end{pmatrix} + \begin{pmatrix} 0 \\ 0 \\ -\dfrac{U_o}{L} \\ \dfrac{I_L}{C} \end{pmatrix} \ddot{\tilde{d}},$$

$$\mathrm{E} = \begin{pmatrix} 0 & 1 & 0 & 0 \\ 0 & 0 & -1 & K+1 \\ 0 & 0 & 0 & -\dfrac{D}{L} \\ 0 & 0 & \dfrac{D}{C} & \dfrac{1}{\mathrm{RC}} \end{pmatrix}, \quad \mathrm{F} = \begin{pmatrix} 0 \\ 0 \\ -\dfrac{U_o}{L} \\ \dfrac{I_L}{C} \end{pmatrix} \tag{12}$$

It is necessary to judge whether the constructed control system is controllable through the controllability matrix $P = (F \;\; FE \;\; FE^2 \;\; FE^3)$. It can be verified that $rank(P^{-1}) = 4$, so the constructed system is controllable.

Assume that the desired poles are $\alpha_1 \pm j\beta_1$ and $\alpha_2 \pm j\beta_2$; $\alpha_1 \pm j\beta_1$ are set as the dominant poles; in order to reduce the influence of nondominant poles $\alpha_2 \pm j\beta_2$ on the approximate second-order system with the dominant pole $\alpha_1 \pm j\beta_1$, $|\alpha_2| > 10|\alpha_1|$ should be satisfied. Assume $\alpha_1 \pm j\beta_1$ and $\alpha_2 \pm j\beta_2$ are the roots of polynomial $(\lambda^2 + 2\omega_{n1}\zeta_1\lambda + {\omega_{n1}}^2)$ and $(\lambda^2 + 2\omega_{n2}\zeta_2\lambda + {\omega_{n2}}^2)$.

According to the empirical formula of the second-order system, $T_s = 4/\omega_{n1}\zeta_1$, and the corresponding relation between damping coefficient ζ_1 and the overshoot P.O. shown in Table 1, the ζ_1, ω_{n1}value can be determined. T_s is the adjustment time required by the system.

According to the Ackerman formula, the state feedback control gain matrix $(K_1 \;\; K_2 \;\; K_3 \;\; K_4)$ could be calculated as follows.

$$\begin{aligned} &(K_1 \;\; K_2 \;\; K_3 \;\; K_4) \\ &= (0 \;\; 0 \;\; 0 \;\; 1)\, P^{-1} \left(E^2 + 2\omega_{n1}\zeta_1 E + {\omega_{n1}}^2 I\right) \\ &\cdot \left(E^2 + 2\omega_{n2}\zeta_2 E + {\omega_{n2}}^2 I\right) \end{aligned} \tag{13}$$

I is the unit matrix, whose order is the same as E. The two-order derivative of the state feedback control law is as follows.

$$\ddot{\tilde{d}} = -K_1 e - K_2 \dot{e} - K_3 \ddot{x}_1 - K_4 \ddot{x}_2 \tag{14}$$

Getting the double integral of $\ddot{\tilde{d}}$, the state feedback control law is as follows.

$$\tilde{d} = -K_1 \int_0^t \int_0^t e\, dt\, dt - K_2 \int_0^t e\, dt - K_3 x_1 - K_4 x_2 \tag{15}$$

According to (15), the program of calculation of switch-on time can be determined. Among these variables, v_ref, i_l, Vi, Vo, K, v_err, err, K1, K2, K3, and K4 denote V_{ref}, i_L, u_i, u_o, K, e_v, e, K_1, K_2, K_3, and K_4, and the variable period is half of the switch period value of DSP. The program is as follows.

```
D = (1 − v_i / v_o);
v_err = v_ref − v_o;
err = (K + 1) ∗ v_err − i_l;
sigma_1+ = err;
sigma_2+ = sigma_1;
duty_delta = −K1 ∗ sigma_2 − K2 ∗ sigma_1 − K3
           ∗ i_l − K4 ∗ v_o;
duty = period ∗ D + duty_delta
```

(16)

3. Simulation with Matlab

By substituting the prototype parameters L = 0.0005H, C = 0.0023F, Ui = 230V, Uo = 385V, R = 37Ω, and I_L = 17.4A into (9), the uncorrected system state equation (17) is as follows.

$$\begin{pmatrix} \dot{x}_1 \\ \dot{x}_2 \end{pmatrix} = \begin{pmatrix} 0 & -800 \\ 173.9 & -11.8 \end{pmatrix} \begin{pmatrix} x_1 \\ x_2 \end{pmatrix} + \begin{pmatrix} -770000 \\ 7573 \end{pmatrix} \tilde{d}, \quad y = (0, 1) \begin{pmatrix} x_1 \\ x_2 \end{pmatrix} \tag{17}$$

The Bode diagram, root locus, and step response of the uncorrected system can be obtained via (17); it is shown in Figure 2. From the Bode diagram shown in Figure 2(a), it can be seen that the amplitude margin is -59.7dB and the phase margin is 144deg. From the root locus shown in Figure 2(b), it can be observed that the system has a zero point in the right half plane, so the system is a nonminimum phase system, whose overshoot will be large. From the local root locus shown in Figure 2(c), it can be discovered that when the gain is greater than 0.001, the characteristic root of the system is located in the right half plane, and then the system is unstable. Figure 2(d) is the open-loop step response of uncorrected system; although it is stable, the steady-state value is close to - 1000V, and the overshoot is large. Figure 2(e) is the closed-loop step response of the uncorrected system, which is unstable.

Table 1: Relationship between damping coefficient ζ_1 and overshoot P.O.

damping ratio ζ_1	0.9	0.8	0.7	0.6	0.5	0.4	0.3
Overshoot P.O. %	0.2	1.5	4.6	9.5	16.3	25.4	37.2

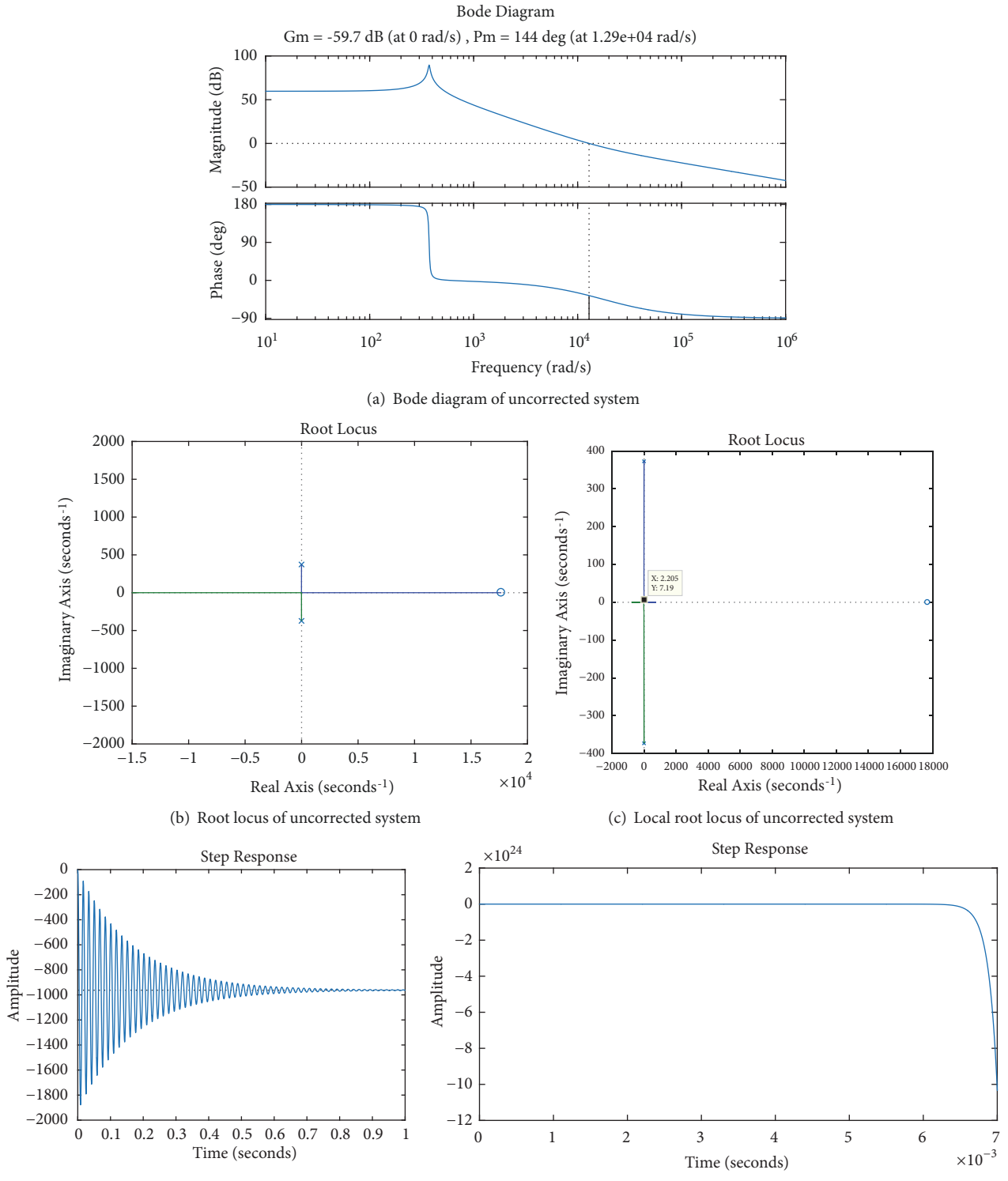

(a) Bode diagram of uncorrected system

(b) Root locus of uncorrected system

(c) Local root locus of uncorrected system

(d) Open-loop step response of uncorrected system

(e) Closed-loop step response of uncorrected system

Figure 2: Bode diagram, root locus, and step response of uncorrected system.

The value of K varies from 0 to 1.414, taking K as disturbance and assuming its value is 1. By substituting the prototype parameters into (12), the state equation with internal model can be constructed as follows.

$$\begin{pmatrix} \dot{e} \\ \ddot{e} \\ \dddot{x}_1 \\ \dddot{x}_2 \end{pmatrix} = \begin{pmatrix} 0 & 1 & 0 & 0 \\ 0 & 0 & -1 & 2 \\ 0 & 0 & 0 & -800 \\ 0 & 0 & 173.9 & -11.8 \end{pmatrix} \begin{pmatrix} e \\ \dot{e} \\ \ddot{x}_1 \\ \ddot{x}_2 \end{pmatrix} + \begin{pmatrix} 0 \\ 0 \\ -770000 \\ 7573 \end{pmatrix} \ddot{\ddot{d}}$$

$$E = \begin{pmatrix} 0 & 1 & 0 & 0 \\ 0 & 0 & -1 & 2 \\ 0 & 0 & 0 & -800 \\ 0 & 0 & 173.9 & -11.8 \end{pmatrix}, \quad F = \begin{pmatrix} 0 \\ 0 \\ -770000 \\ 7573 \end{pmatrix} \tag{18}$$

P could be calculated as follows.

$$P = \begin{pmatrix} F & FE & FE^2 & FE^3 \end{pmatrix} = \begin{pmatrix} 0 & 0 & 0.000000078514600 & -0.000026156887720 \\ 0 & 0.000000078514600 & -0.000026156887720 & -0.011231602427096 \\ -0.000000077000000 & -0.000000605840000 & 0.010705091088000 & 0.210604535638400 \\ 0.000000000757300 & -0.000013381363860 & -0.000263255669548 & 1.858508923302534 \end{pmatrix} \tag{19}$$

It can be easily verified that rank (P^(−1)) = 4, so the system function is controllable.

Table 1 is the corresponding relationship between the damping coefficient and the overshoot P.O when the system has no zero point in the right half plane. On the contrary, the overshoot is often larger than those shown in Table 1. After correcting, the step response of closed-loop and Bode diagram can be observed when the damping coefficients ζ_1 are 0.7, 0.9, 1.2, 1.5, 1.8, and 2, respectively, and $\omega_{n1} = 10$, $|\omega_{n2}\zeta_2| = 10|\omega_{n1}\zeta_1|$. The improved effects are shown in Figure 3; as the damping coefficient increases, the amplitude margin and the phase margin increase accordingly in Figure 3(a), while the overshoot decreases in Figure 3(b).

When $\zeta_1 = 2$, both the amplitude margin and phase margin are reasonable, the overshoot of step response is less than 20%, and the adjustment time is less than 2s. When $\zeta_1 = 2$, $\omega_{n1} = 10$, and $|\omega_{n2}\zeta_2| = 10|\omega_{n1}\zeta_1|$, Q can be calculated as follows.

$$Q = (E^2 + 40 * E + 100 * I) * (E^2 + 400 * E + 10000 * I) \tag{20}$$

According to (13), the coefficients of state variables feedback gain matrix are as follows.

$$\begin{pmatrix} K_1 & K_2 & K_3 & K_4 \end{pmatrix} = \begin{pmatrix} -0.003692304056808 & -0.001635317766189 & -0.000578675009682 & 0.000821370994958 \end{pmatrix} \tag{21}$$

The corrected system is shown in Figure 4(a), the syso and K_{Gain} are regarded as an open-loop transfer function and a gain, respectively. In practical control, when the value of e_v is greater than 30V, its amplitude is limited to 30V, and the value of K+1 is less than or equal to 2.414, so the value of K+1—I_L is less than 2.414, and the value of K_{Gain} is less than 72V. The root locus and the local root locus are shown in Figure 4(b). From the local root locus, it can be seen that when the gain exceeds 75, the corrected system remains stable.

4. Experiment Results

A 4 kW digital totem pole PFC prototype is shown in Figure 5.

Under different input voltage and output power conditions, the waveforms of input voltage and input current are

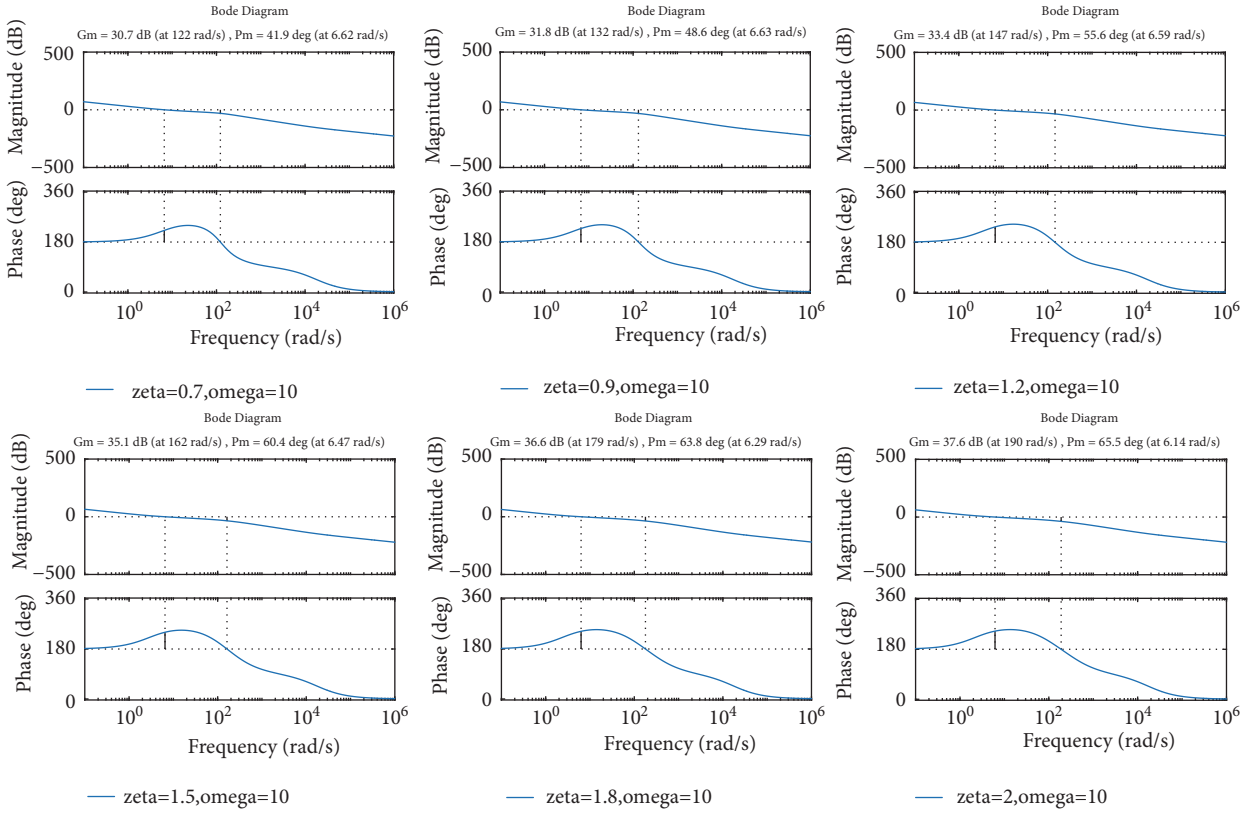

(a) Bode diagrams of different damping coefficient ζ_1

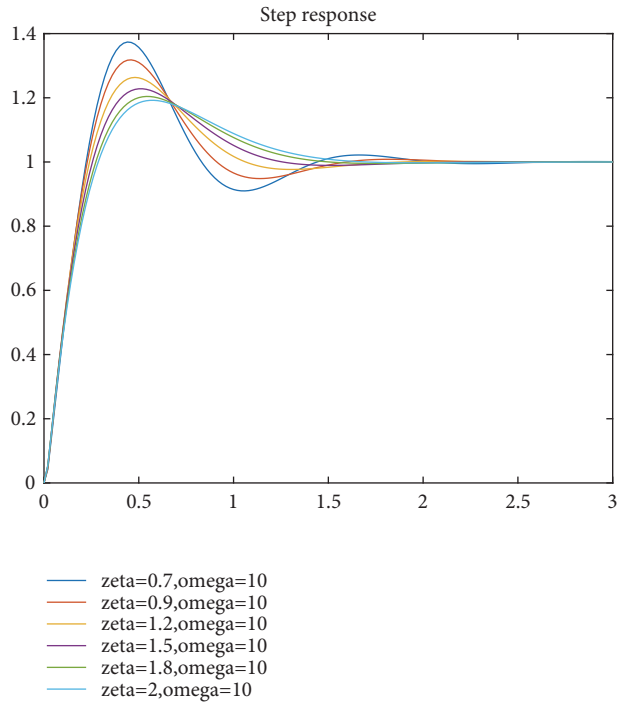

(b) Step responses of different damping coefficient ζ_1

FIGURE 3: Bode diagrams and step responses of different damping coefficient ζ_1.

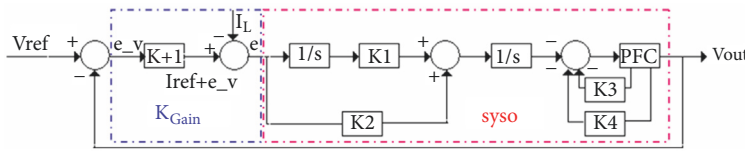

(a) Corrected system

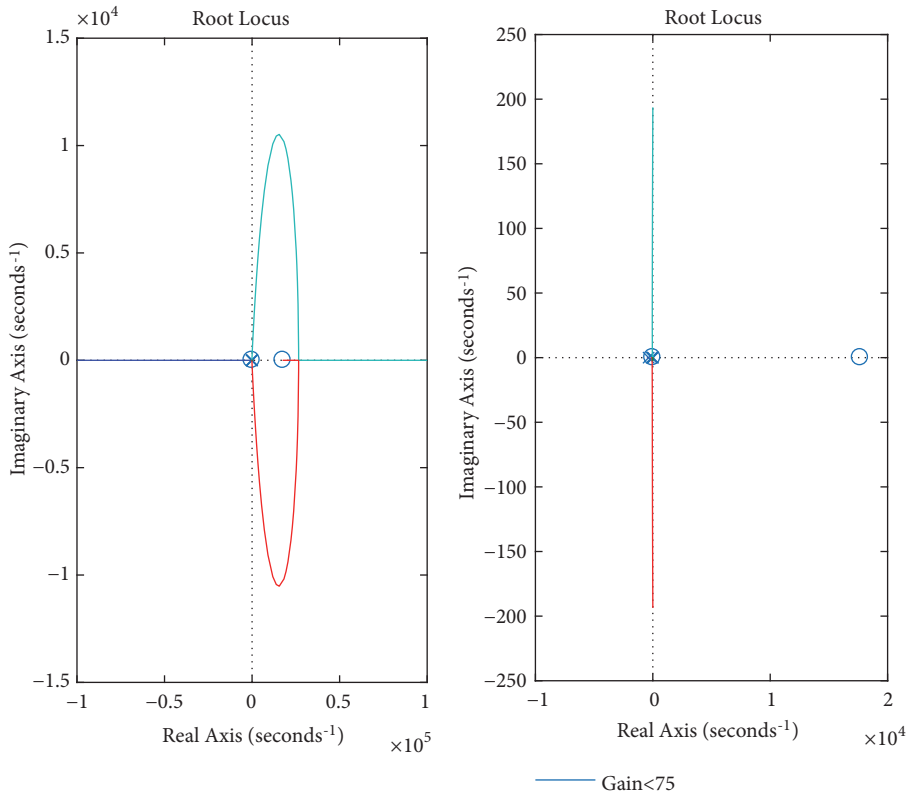

(b) Root locus and local root locus of corrected system

Figure 4

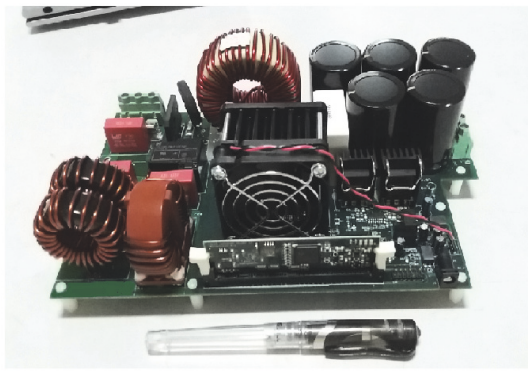

Figure 5: An 4 kW digital totem pole PFC prototype.

shown in Figure 6. It can be observed that the higher the input voltage and output power, the better the input current. As shown in Figure 6(a), when the input voltage is 115 V and the output power is 2 kW, the RMS and peak-to-peak value of the input current are 17.88 A and 61.2 A, respectively. As shown in Figure 6(b), when the input voltage is 230V and the output power is 4 kW, the RMS and peak-to-peak value of the input current are 17.47 A and 55.6 A, respectively.

The test results of efficiency and power loss are shown in Figure 7(a). As the input voltage increases, the efficiency increases and the power loss decreases. The peak efficiency is 99.02% (230V) and 98.08% (115V) when the switching frequency is 66 kHz. As shown in Figure 7(b), when the load is more than half, the THD is below 4% regardless of whether the input voltage is 115V or 230V. The minimum THD values are 2.8% (115 V) and 2.6% (230 V), respectively.

5. Conclusion

Using GaN HEMTs as switching device, a prototype of 4 kW digital noninterleaved totem pole PFC based on state variable feedback control with internal model is introduced in detail in this paper. Due to the advantages of control method

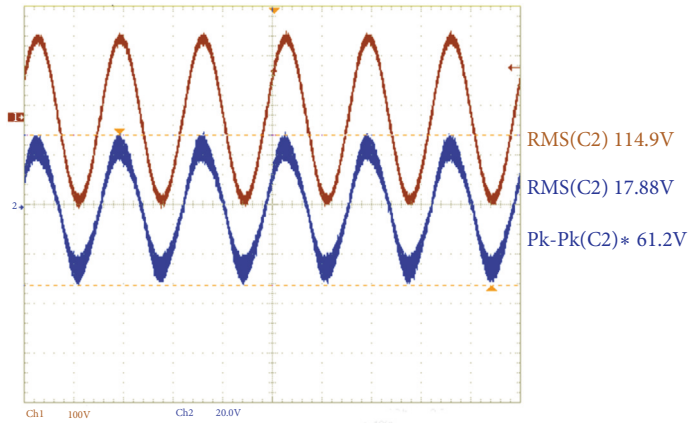

(a) Vi=115 V, P=2 kW

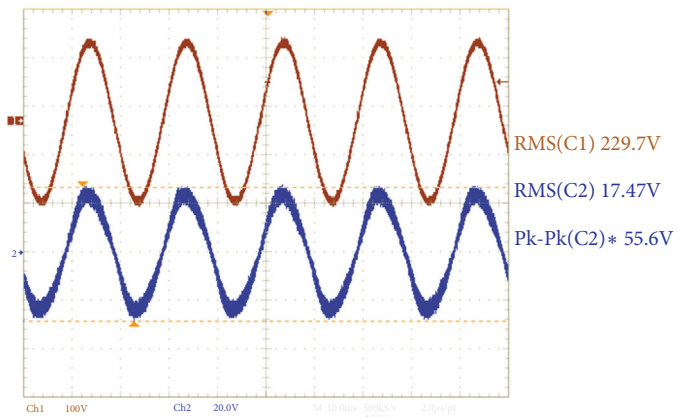

(b) Vi=230 V, P=4 kW

Figure 6: The test waveforms of input voltage and input current.

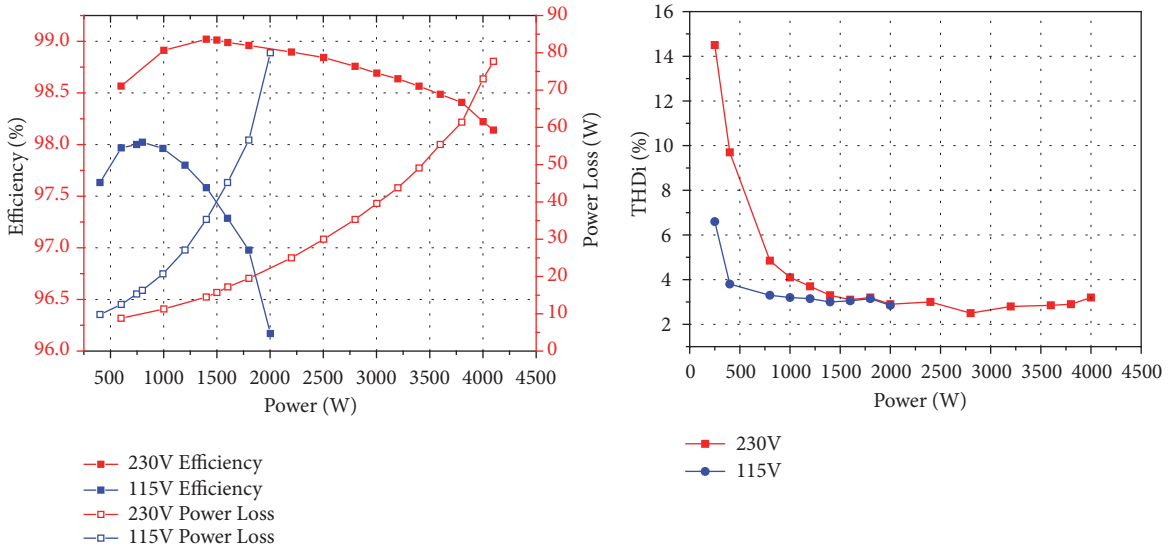

(a) The test results of efficiency and power loss

(b) The test results of THD

Figure 7: The test results of efficiency and power loss and THD.

and GaN HEMT, the prototype achieves better performances such as efficiency, power loss, THD related to EMI, compact structure, and higher power density than the PFC based on traditional PI control with Si MOSFETs. Noninterleaved structure effectively reduces the number of devices and the cost of filtering. Therefore, the cost of totem pole PFC with GaN HEMT is not higher than the traditional PFC with Si MOSFET. It should be noted that PFC with GaN HEMT has obvious advantages in efficiency only when it works in hard switching mode of CCM, not in DCM and CRM mode. Soft switching can be achieved in DCM and CRM with Si MOSFET, and the switching loss is not large in this case. But no matter whether in CCM or DCM and CRM, PFC with GaN HEMTs achieves better performances in EMI than the one with Si MOSFETs.

Data Availability

The data used to support the findings of this study are included within the article.

Conflicts of Interest

The authors declare that there are no conflicts of interest regarding the publication of this paper.

Acknowledgments

This work was supported by the Science and Technology Projects of Guizhou Province of China (Grant No. 2014LH7050) and the Science and Technology Projects of Guizhou Education Department (Grant No. QianJiaoKe 2010018).

References

[1] F. Gao and Y. Feng, "Digital non-interleaved high-power totem pole PFC based on double integral sliding mode," *IEICE Electronics Express*, vol. 15, no. 8, pp. 1–9, 2018.

[2] M. Jamshidi, *Design of Intelligent Manufacturing Systems*, Prentice Hall, Upper Saddle River, N.J, USA, 1998.

[3] C. T. Chen, *Linear System Theory and Design*, Oxford University Press, New York, NY, USA, 3rd edition, 1999.

[4] C. E. Rohrs, J. L. Melsa, and D. Schultz, *Linear Control Systems*, McGraw-Hill, New York, NY, USA, 1993.

[5] E. W. Kamen and B. S. Heck, *Fundamentals of Signals and Systems Using MATLAB*, Prentice Hall, Upper Saddle River, N.J, USA, 1997.

[6] G. Goodwin, S. Graebe, and M. Salgado, *Control System Design*, Prentice Hall, Saddle River, N.J., USA, 2001.

[7] G. F. Franklin, J. D. Powell, and A. Emami-Naeini, *Feedback Control of Dynamic Systems*, Prentice Hall, Upper Saddle River, N.J, USA, 4th edition, 2002.

[8] R. E. Kalman and R. S. Bucy, "New results in linear filtering and prediction theory," *Transactions of the American Society of Mechanical Engineering, Series D, Journal of Basic Engineering*, 1961.

[9] R. E. Kalman, "Mathematical description of linear dynamical systems," *Journal of the Society for Industrial & Applied Mathematics, Series A: Control*, vol. 1, no. 2, pp. 152–192, 1963.

[10] R. E. Kalman, "A new approach to linear filtering and prediction problems," *Journal of Basic Engineering*, 1960.

[11] J. B. Burl, *Linear Optimal Control*, Prentice Hall, Upper Saddle River, NJ, USA, 1999.

[12] L. Balogh and R. Redl, "Power-factor correction with interleaved boost converters in continuous-inductor-current mode," in *Proceedings of the 8th Annual Applied Power Electronics Conference and Exposition*, pp. 168–174, 1993.

[13] B. A. Miwa, *Interleaved conversion techniques for high density power supplies [Ph.D. dissertation]*, Massachusetts Institute of Technology. Dept. Elect. Eng. Comput. Sci., 1992.

[14] B. Miwa, D. Otten, and M. Schlecht, "High efficiency power factor correction using interleaving techniques," in *Proceedings of the APEC '92 Seventh Annual Applied Power Electronics Conference and Exposition*, pp. 557–568, Boston, MA, USA, 1992.

[15] R. Giral, L. Martinez-Salamero, and S. Singer, "Interleaved converters operation based on CMC," *IEEE Transactions on Power Electronics*, vol. 14, no. 4, pp. 643–652, 1999.

[16] J. Maixe, R. Leyva, L. Martinez-Salamero, and R. Giral, "Sliding-mode control of interleaved boost converters," *IEEE Transactions on Circuits and Systems I: Fundamental Theory and Applications*, vol. 47, no. 9, pp. 1330–1339, 2000.